# Single-crystal, mesoscopic films of lead zinc niobate-lead titanate: Formation and micro-Raman analysis

Jonathan E. Spanier
*Department of Applied Physics and Applied Mathematics, Columbia University, New York, New York 10027*

Miguel Levy[a)]
*Departments of Physics and Materials Science and Engineering, Michigan Technological University, Houghton, Michigan 49931*

Irving P. Herman and Richard M. Osgood, Jr.
*Department of Applied Physics and Applied Mathematics, Columbia University, New York, New York 10027*

Amar S. Bhalla
*Department of Materials Science and the Materials Research Laboratory, Penn State University, College Park, Pennsylvania 16802*

(Received 5 March 2001; accepted for publication 6 July 2001)

A process to form thin films of lead zinc niobate–lead titanate (PZN–PT) from a bulk crystal for microelectronic and microelectromechanical device applications is presented. The structural phase transitions and ferroelectric ordering in unpoled crystalline bulk and thin-film relaxor PZN–PT are studied from $-190\,^{\circ}\mathrm{C}$ to $600\,^{\circ}\mathrm{C}$ using polarized micro-Raman scattering. The structural phase transitions in this material are observed by distinct changes in the polarization selectivity. The results for the thin film and bulk crystal are in good agreement for a wide range of the temperatures studied, indicating that the thin-film PZN–PT retains much, if not all, of the structural and ferroelectric properties of the original bulk substrate. © *2001 American Institute of Physics.* [DOI: 10.1063/1.1397761]

Single crystal $(1-x)\mathrm{Pb}(\mathrm{Zn}_{1/3}\mathrm{Nb}_{2/3})\mathrm{O}_3$-$x\mathrm{PbTiO}_3$ (PZN–PT) is a relaxor ferroelectric material of considerable interest.[1] Its high electromechanical coupling and piezoelectric response are superior to the $\mathrm{PbZrO}_3$–$\mathrm{PbTiO}_3$ solid solution system used over the last 40 years for transducer applications.[2,3] Its materials characteristics are also more temperature insensitive than those in normal ferroelectrics. These properties collectively make PZN–PT an attractive material for use in ultrasonic transducers and piezoelectric actuator devices. However, the molten flux method used to fabricate single-crystal PZN–PT yields macroscopically thick crystals. For this reason, the development of fabrication techniques to produce single-crystal PZN–PT films is of considerable technological interest for integrated systems.

The fabrication of mesoscopic ($\sim 1-10\,\mu$m thick) PZN–PT films possessing characteristics comparable to the bulk material is important for on-chip applications, such as microactuators and valves for microfluidic channels, and microelectromechanical devices. We use a crystal ion slicing technique to detach thin layers from PZN–PT. A crucial question in the application of ion slicing is the persistence of the same type of ferroelectric structure in the material. Polarized Raman scattering has been shown to be an effective means of studying ferroelectric phase transitions in both normal and relaxor ferroelectric crystals such as PZN–PT.[4] The appearance and intensity of normally silent (inactive) Raman modes and the extent to which polarization selectivity in Raman scattering is observed are indications of local variations in the ferroelectric nanodomains, or long-range ferroelectric ordering. A comparison of the Raman scattering spectral response of PZN–PT bulk and film materials is thus of interest because it can shed light on the effect of processing and dimensional factors on the dynamics responsible for the strong piezoelectric character of this material system.

The unique properties of relaxor ferroelectrics are still not very well understood and considerable effort is being devoted to the study of the cluster and nanoregion dynamics responsible for the strong polar–strain coupling in these materials.[5,6] Since the crystalline quality and differences in structural and ferroelectric phases can affect the Raman peak position, linewidth and polarization selectivity, temperature-dependent polarized micro-Raman scattering was performed to compare these parameters in the film and bulk. The present work shows that the Raman results in the film and in bulk are similar, demonstrating that the energetic ion implantation used to process the films has no deleterious effect in the ferroelectric phases of the material.

Single-crystal PZN–4.5% PT samples were grown by the flux method described elsewhere[3] and will be referred to as ''bulk.'' The crystalline phase purity was confirmed by x-ray diffraction, and the samples were determined to be (001) oriented. Mesoscopic films of PZN–PT ($\sim 7\,\mu$m) were prepared from bulk crystalline (001)-PZN–PT wafers by slicing a thin layer off the top of the sample flat. This technique, known as crystal ion slicing, has been applied to other metal oxides and is described in detail elsewhere.[7] The technique relies on the formation of a sacrificial layer below the surface. Singly charged 3.8 MeV helium ions are implanted 5° off normal to the surface of the PZN–PT bulk sample without masking, to a total implant dose of $5\times 10^{16}$ ions/cm$^2$. Helium is chosen as the implantation species because of its small atomic mass, thus yielding a deeply

a)Electronic mail: mlevy@mtu.edu

 

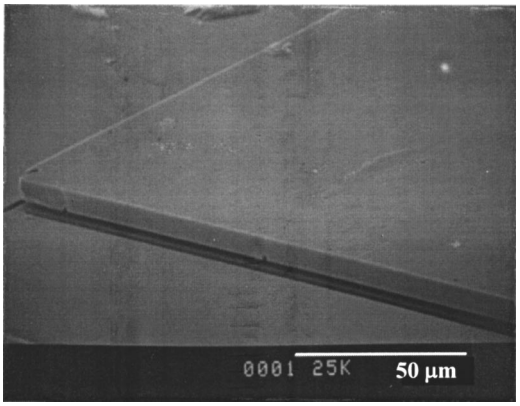


FIG. 1. Scanning electron micrograph of partially detached PZN–PT film and substrate using crystal ion slicing is shown.

buried damage layer. The samples are mounted on a specially designed, two-inch diameter water-cooled target holder and the temperature of the substrate is maintained below 400 °C. As an added precaution, the beam current during the implant is kept low ($<0.25\,\mathrm{mA/cm^2}$) and the uniformity of the implantation is checked by four Faraday cups outside the target holder.

After implantation, the sample is annealed at 600 °C for 40 s and immersed in a 37% dilution of hydrochloric acid for 5 h to detach the thin films. This procedure yields a sacrificial-layer etch rate of $\sim 100\,\mu$m/h/facet. Free-standing 1 mm$^2$ films are obtained and transferred to a glass slide with the help of a micromanipulator for testing. The bonding of film to glass is by van der Waals forces. Postimplantation annealing is absolutely necessary to activate the large etch selectivity ($\gtrsim 500{:}1$) between the sacrificial layer and the rest of the sample. The role of this postimplantation anneal on the sacrificial layer microstructure is presently under investigation and will be reported on in the future.

After separation from the bulk, the sample was examined with both optical and electron microscopy. Figure 1 shows a scanning electron micrograph of a partially detached film after 2 h in the etchant. In line with other oxide materials etched with ion slicing techniques, the sample surface was smooth and free of defects. Further, the sample edges were clearly defined with no sign of stress induced damage. Separate experiments from those described here have confirmed that the samples are piezoelectric.[8]

In order to examine the ferroelectric character of the ion sliced sample more exactly, we undertook Raman measurements of the vibrational properties. Polarized Raman scattering was collected over the range from 150 to 1000 cm$^{-1}$ using the 488.0 nm line of an Ar-ion laser focused to a spot of approximately 2 $\mu$m in diameter. The Raman spectra were calibrated with the use of plasma lines from the Ar-ion laser, and the accuracy and resolution of the Raman spectra were better than 1 cm$^{-1}$. For the bulk sample, the spectra were taken in the backscattering configurations $z(x,x)\bar{z}$, $z(x,y)\bar{z}$, $z(x',x')\bar{z}$, and $z(x',y')\bar{z}$, where $x$, $y$, $x'$ and $y'$ refer to the $\langle 100\rangle$, $\langle 010\rangle$, $\langle 110\rangle$, and $\langle 1\bar{1}0\rangle$ directions, respectively. For the thin film, the spectra were taken in the backscattering configuration $z(x'',x'')\bar{z}$ and $z(x'',y'')\bar{z}$, where $x''$ and $y''$ are perpendicular but otherwise undefined in the plane of the sample. $z(x,x)\bar{z}$, $z(x',x')\bar{z}$, and $z(x'',x'')\bar{z}$ are referred to as

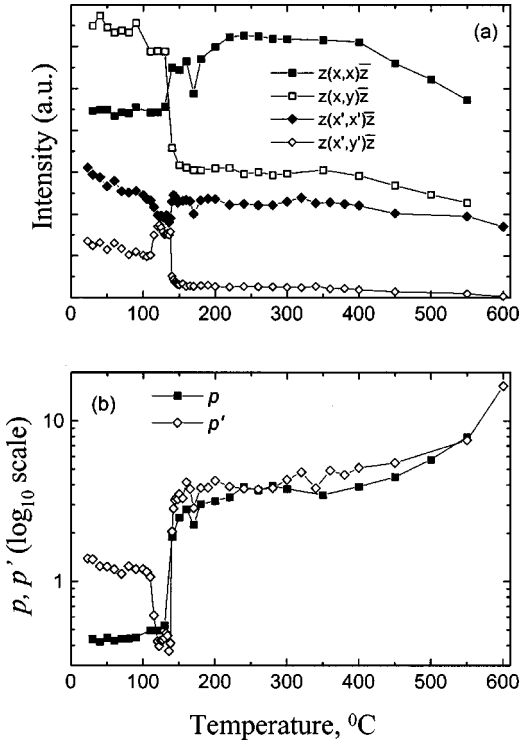


FIG. 2. (a) Raman scattering intensities of the $\sim 780\,\mathrm{cm^{-1}}$ line for the bulk sample for the $z(x,x)\bar{z}$, $z(x,y)\bar{z}$, $z(x',x')\bar{z}$, and $z(x',x')\bar{z}$ configurations, and the polarization ratios $p$ (solid squares) and $p'$ (open diamonds) plotted as functions of temperature are shown. The intensities are offset for clarity, and the polarization ratios are on a log scale.

parallel configurations and $z(x,y)\bar{z}$, $z(x',y')\bar{z}$, and $z(x'',y'')\bar{z}$ as perpendicular. Care was taken to ensure that the laser was not heating the sample by confirming that the peak linewidths and positions did not depend on the incident laser power intensity for the range used. All reported peak intensities, positions, and linewidths are the result of Lorentzian fitting. Measurements were performed on the bulk crystal and thin film at selected temperatures from 23 °C to 600 °C in both temperature upstroke and downstroke after earlier temperature cycling to 600 °C to ensure that the samples were not poled. Measurements were also performed on the unpoled bulk crystal and unpoled thin film at selected temperatures in the range from −190 °C to 23 °C in temperature downstroke. The sample temperature was controlled to within ±0.1 °C by a Linkam THMS 600 heating/cooling stage. Care was taken to ensure that each spectrum was stable following a controlled change in temperature.

In the room temperature (RT) polarized Raman spectra from both the unpoled PZN–PT film and the unpoled bulk, distinct broad peaks are observed near 270, 590, and 780 cm$^{-1}$ with additional weak peaks, one near 420 cm$^{-1}$ and another near 490 cm$^{-1}$. The Raman signal for each configuration is stable over time and does not vary spatially for either the bulk or the film. The unpolarized ($z(x'',x''+y'')\bar{z}$ and $z(x',x'+y')\bar{z}$) peak position and linewidth of the film and the bulk are nearly identical ($\omega_{\mathrm{film}}=777.1$, $\Gamma_{\mathrm{film}}=83$, $\omega_{\mathrm{bulk}}=776.4$, and $\Gamma_{\mathrm{bulk}}=79\,\mathrm{cm^{-1}}$). There is not much variation in the peak position with temperature and the linewidth increases slightly with temperature. This is consistent with the results found in 9% PT material,[4] and also with those of Gupta *et al.*[9] who examined 2%, 8.5%, and 11% PT material.

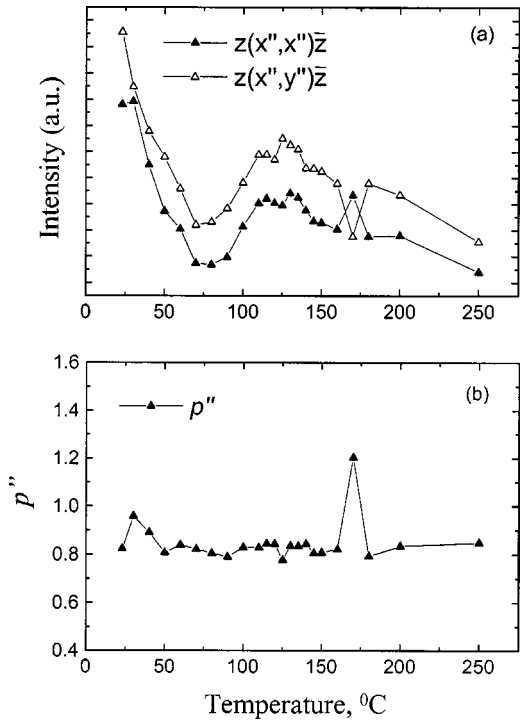


FIG. 3. (a) Raman scattering intensity of the $\sim 780\ \mathrm{cm}^{-1}$ line for the film for the $z(x'',x'')\bar{z}$ and $z(x'',y'')\bar{z}$ configurations, and (b) the polarization ratio $p''$ plotted as functions of temperature are shown.

We define the polarization ratios $p$, $p'$, and $p''$ to be the ratios of intensities in the parallel $[z(x_i,x_i)\bar{z}]$ to perpendicular $[z(x_i,y_i)\bar{z}]$ polarizations for each coordinate system. Figure 2(a) shows the intensities of the $\sim 780\ \mathrm{cm}^{-1}$ line for each of the configurations, and Fig. 2(b) the values of $p$ and $p'$ on a log scale, both for the bulk sample in temperature upstroke. The Raman intensity and polarization selectivity ratio $p''$ from the unpoled thin film are shown as functions of temperature for this peak in Fig. 3(a) and 3(b), respectively. As seen in Fig. 2(b), the polarization ratios $p$ and $p'$ undergo changes above 130 °C. Distinct changes in $p$ and $p'$ with temperature correspond to the cubic–tetragonal ($\sim$168 °C) and tetragonal–rhombohedral ($\sim$136 °C) transitions, which are consistent with measurements in 4.5% PT material by other means.[10] (The strong feature near 110 °C in $p'$ is due to the tetragonal–rhombohedral transition in the host PZN lattice.) Since the same polarization ratio changes are seen for $p$ and $p'$, such measurements could be made with any choice of normal axes, such as those for $p''$. While the variations in the intensity and polarization selectivity in the film (Fig. 3) are different from the bulk, there is a strong feature near 170 °C and a weak feature near 140 °C that indicate the presence of phase transitions. Both these features are reproducible after thermal cycling and from film to film, and much bigger than the noise of the measurements. Specifically, the intensity in both configurations decreases slightly near 140 °C and the parallel and perpendicular intensities increase and decrease, respectively, near 170 °C. The fitted peak position and linewidth are similar in the film and bulk at temperatures from −190 °C to 23 °C (not shown).

The Raman lines and phonon symmetries in PZN–PT have been tentatively assigned in Refs. 4 and 11 and are not discussed here. The appearance of Raman lines above the tetragonal to cubic phase transition in PZN–9% PT have been attributed to the presence of nanodomains having symmetry Fm3m in a crystal of Pm3m symmetry.[4] The observed changes in the polarization selectivity $p$ and $p'$ near 400 °C and above are explained by a randomly oriented local polarization that is expected to develop at this temperature.[12] All these features are observed in both film and bulk samples studied, indicating the same ferroelectric structure in both.

Differences in the variation of the peak intensity and polarization selectivity of the bulk and the film (Figs. 2 and 3, respectively) and slight differences ($<2\ \mathrm{cm}^{-1}$) in their peak energy and width below RT may be due to the presence of residual defects resulting in domain pinning caused by the implantation. This could be studied by post-detachment annealing to repair this possible damage. Still, the polarization selectivity indicates that the structural phase transitions in the film and the bulk occur at approximately the same temperatures. In addition, the RT peak position and width of the $\sim 780\ \mathrm{cm}^{-1}$ peak in the film and bulk are nearly identical. This indicates that the process of forming mesoscopic PZN–PT films from bulk does not appear to affect the mechanism driving the ferroelectric phase transition in the material. Moreover, the piezoelectric performance of the mesoscopic film material is comparable to bulk PZN–PT, as will be reported elsewhere.[8]

A method for preparing mesoscopic films of PZN–PT has been presented, along with an investigation of the structure of these films and bulk PZN–PT by Raman scattering. The process may allow high-quality epitaxially thin films of PZN–PT and related materials to be easily integrated into microelectromechanical systems and other microelectronic devices. Temperature-dependent, polarized micro-Raman scattering has been shown to be an effective probe of both the structural and ferroelectric phases, and demonstrates that the film retains the same composition and much of the structural quality of the bulk crystal from which it was processed.

The authors thank Professor H. Bakhru of SUNY at Albany for the ion implantation. This work was supported by NSF Grant No. ECS-9980828 (M.L. and R.M.O.), Joint Services Electronics Program (JSEP) Contract No. DAA-G05S-97-0166 and the shared experimental facilities of the NSF MRSEC under Award No. DMR-9809687.

[1] J. Kuwata, K. Uchino, and S. Nomura, Ferroelectrics **37**, 579 (1981); Jpn. J. Appl. Phys., Part 1 **21**, 1298 (1982).
[2] S.-E. Park and T. R. Shrout, J. Appl. Phys. **82**, 1804 (1997).
[3] S.-E. Park, M. L. Mulvihill, G. Risch, and T. R. Shrout, Jpn. J. Appl. Phys., Part 1 **36**, 1154 (1997).
[4] F. Jiang and S. Kojima, Jpn. J. Appl. Phys., Part 1 **38**, 5128 (1999).
[5] P. M. Gehring, S. E. Park, and G. Shirane, Phys. Rev. Lett. **84**, 5216 (2000).
[6] C. A. Randall and A. S. Bhalla, Jpn. J. Appl. Phys., Part 1 **67**, 6405 (1990).
[7] M. Levy, R. M. Osgood, R. Liu, L. E. Cross, G. S. Cargill, A. Kumar, and H. Bakhru, Appl. Phys. Lett. **73**, 2293 (1998).
[8] S. Gupta, R. S. Katiyar, and A. S. Bhalla, Ferroelectrics **29**, 75 (2000).
[9] M. Levy, A. Bandyopadhyay, and K. Moon (unpublished).
[10] J. Kuwata, K. Uchino, and S. Nomura, Ferroelectrics **37**, 579 (1981).
[11] S. Gupta, R. S. Katiyar, R. Guo, and A. S. Bhalla, J. Raman Spectrosc. **31**, 921 (2000).
[12] G. Burns and F. H. Dacol, Phys. Rev. B **28**, 2527 (1983); Solid State Commun. **48**, 853 (1983).